Meteoric ice contribution and influence of weather on landfast ice growth in the Gulf of Finland, Baltic Sea

Jari UUSIKIVI,[1] Mats A. GRANSKOG,[2,3] Eloni SONNINEN[4]

[1]*Department of Physics, University of Helsinki, PO Box 64, FIN-00014 Helsinki, Finland*
E-mail: jari.uusikivi@helsinki.fi
[2]*Arctic Centre, University of Lapland, PO Box 122, FIN-96101 Rovaniemi, Finland*
[3]*Norwegian Polar Institute, Polar Environmental Centre, NO-9296 Tromsø, Norway*
[4]*Dating Laboratory, University of Helsinki, PO Box 64, Gustaf Hellströmin Katu 2,*
FIN-00014 Helsinki, Finland

ABSTRACT. The stable oxygen isotopic composition ($\delta^{18}O$), texture and stratigraphy of landfast ice in Santala Bay, Gulf of Finland, were studied annually from 1999 to 2009. Apart from one year when there was no ice, maximum ice thickness ranged from 0.22 to 0.60 m. Maximum ice thickness was determined primarily by average air temperature, and a simple accumulated freezing-degree-day–ice-thickness model explained 86% of ice-thickness variance. The total ice thickness each winter was dominated by columnar ice and intermediate granular/columnar ice formed at the base of the ice cover. Meteoric ice (snow ice and superimposed ice) accumulated at the top of the ice cover each winter and constituted 4–39% of the total ice thickness (ice mass). Snow ice formed in seven of the ten winters; superimposed ice formed in only three winters. The snow fraction in the meteoric ice contributed 1–30% annually of the total ice mass, with an average of 8.8%.

INTRODUCTION

Sea ice covers large areas of the Baltic Sea every winter, and the ice-cover season lasts for 5–7 months in the northernmost parts of the Bay of Bothnia. The ice cover has a large impact on navigation and biology, and sea-ice texture and ice-growth mechanisms are important factors controlling key ice parameters such as mechanical strength, and chemical and biological properties. Although the Baltic Sea is a brackish water basin, the ice texture has sea-ice-like features such as brine pockets and irregular crystal boundaries (Kawamura and others 2001). Consequently, we refer to sea ice rather than brackish ice.

Snow-ice and superimposed-ice layers accumulate at the sea-ice surface and are referred to as meteoric ice because of the role of snow and rain in their formation. Snow ice is a mixture of snow and sea water. Superimposed ice is completely or mainly composed of snow meltwater and/or frozen rain. The snow ice in the Baltic Sea was first reported by Palosuo (1963). In the Baltic Sea, depending on season and year, meteoric ice may contribute almost half of the total thickness and up to 35% of the total mass of landfast ice (Granskog and others, 2003, 2004). On landfast ice, superimposed-ice layers can grow at least 0.10–0.15 m thick, and during spring the whole snow cover can be transformed into a superimposed-ice layer (Granskog and others, 2006).

Here we report on landfast ice observations in Santala Bay, Gulf of Finland, spanning an 11 year annual sampling period, 1999–2009. Observations are used to infer the contribution of different ice-growth processes, and especially meteoric ice, to the total mass balance of sea ice in the region. The winter (January–March) North Atlantic Oscillation (NAO) correlates well with Baltic Sea ice-cover extent (Vihma and Haapala, 2009) and, for the first time, we relate Santala Bay ice properties to mean weather conditions in the region.

MATERIAL AND METHODS

Sampling

Ice samples were recovered with an ice corer from coastal fast ice in Santala Bay (59°53.43′ N, 23°06.25′ E), a sheltered, semi-enclosed bay on the southern coast of Finland. With the exception of 2008, when there was no ice to sample, one sample per ice season was collected in early or mid-March between 1999 and 2009. Ice thickness at the measurement site typically reaches a maximum in mid-March (Granskog and others, 2004), so ice samples can be considered to represent most of the ice growth each season. Ice-core stratigraphy and $\delta^{18}O$ data from 1999 to 2001 have been published previously (Granskog and others, 2004).

After collection the ice samples were stored in sealed plastic tubing in a freezer at –20°C. Snow, and sea-water samples from under the ice, at the coring sites were stored in a similar manner. Ice cores were then cut vertically in half in the cold laboratory, and one side was analyzed for texture and stratigraphy using vertical thin sections illuminated between crossed polarizing filters.

Two basic ice textures were present: *columnar*, representing congelation ice formed by freezing of water at the bottom of the ice cover, and *granular*, representing snow ice and superimposed ice accumulated at the top of the ice cover. These two meteoric ice types were subsequently distinguished from each other on the basis of their snow fractions, as described below. A third, intermediate granular/columnar (g/c) texture was also recorded; it is believed to be the result of either higher growth velocities or turbulent conditions at the bottom of the ice cover (Eicken and Lange, 1989). No frazil ice was observed.

Determining oxygen isotopic composition

The other half of the ice core was used to analyze the stable oxygen isotopic composition of ice layers selected on the basis of texture and stratigraphy (Granskog and others,

Table 1. Columnar ice and under-ice sea-water $\delta^{18}O$ values.

Year	Ice $\delta^{18}O$	Water $\delta^{18}O$
1999	−6.37	−8.69
2000	−6.26	−8.69
2001	−5.88	−7.53
2002	−5.96	−8.48
2003	−5.33	−7.46
2009	−5.92	−7.85

2003). These sections were melted in airtight containers at room temperature, as were the snow and frozen sea-water samples. The water samples (0.5 mL) were equilibrated for at least 24 hours at 25°C with CO_2, which was then introduced to a mass spectrometer (Delta^{Plus}XL, Thermo Scientific, Bremen, Germany) to measure the $^{18}O/^{16}O$ isotope ratio. The results are expressed as a $\delta^{18}O$ value in per mil (‰), which is the relative deviation between the isotope ratios of the sample and the international reference Vienna Standard Mean Ocean Water (V-SMOW).

Snow fraction determination

The $\delta^{18}O$ data were used to determine the fraction of snow (or rain) in the snow-ice and superimposed-ice layers, and in the total ice thickness. Lange and others (1990) developed a model to determine the fraction of snow in sea ice, and Jeffries and others (1994) simplified this model to the form used here:

$$f_s + f_{sw} = 1, \tag{1}$$

$$f_s \delta_s + f_{sw} \delta_{sw} = \delta, \tag{2}$$

where f_s is the snow fraction in meteoric ice, f_{sw} is the sea-water fraction of the sample, δ_s and δ_{sw} are the $\delta^{18}O$ values of snow and sea water, respectively, and δ is the $\delta^{18}O$ value of the sample. For δ_s we use the measured snow $\delta^{18}O$ value from each sampling site, excluding any freshly fallen new snow. For those years when snow samples were not available, either because they were lost or no snow was present on the ice, an average δ_s value from other measurements in the area is used. For each year, the measured δ_{sw} is used, except for 2004–06 because those sea-water samples were lost during storage. In those cases, δ_{sw} is derived from the columnar-ice $\delta^{18}O$ value. In Santala Bay, the columnar ice preserves the sea-water $\delta^{18}O$ value (Table 1) in a manner similar to that observed by Macdonald and others (1999) in the Arctic Ocean. Isotopic fractionation was found to be ∼2‰ during columnar ice growth, i.e. columnar ice $\delta^{18}O$ value $\delta_{ci} = \delta_{sw} + 2$‰.

Granular ice layers were divided into snow ice and superimposed ice based on f_s values according to Granskog and others (2004). Superimposed-ice layers were identified as those with $f_s \geq 0.65$. Snow-ice layers were identified as those with $0.65 > f_s \geq 0$. Note that using the snow fraction to classify ice types is different from practice elsewhere (e.g. Antarctica (Lange and others, 1990, Eicken and others, 1994; Jeffries and others, 1994, 1997)), so the amounts of snow ice and superimposed ice and their snow fractions described here are not directly comparable with those elsewhere.
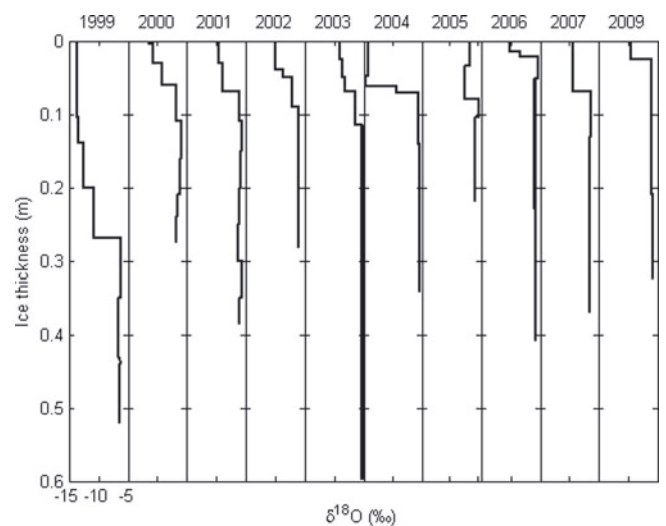

Fig. 1. Ice-core $\delta^{18}O$ profiles for all the years with ice cover from 1999 to 2009. There was no ice in 2008.

Weather observations

Weather data were collected with an automatic weather station at the Tvärminne Zoological Station, located 10 km southeast of the ice-sampling site. Temperature and precipitation data were collected at 30 min intervals between 1999 and 2009. Wind data were collected at the same intervals from December 2001 onwards. Daily average temperatures were used to calculate monthly accumulated freezing degree-day (FDD) values (e.g. 2 days with an average temperature of −1°C gives an FDD value of 2). We also calculated average values for each December, January and February during 1999–2009 (temperature, precipitation) and 2001–09 (wind), 11 year and 9 year average values for each of the three months, and monthly anomalies (the deviation from the 11 year and 9 year average monthly values of the average value for each month). The NAO index, obtained from the US National Oceanic and Atmospheric Administration (http://www.cpc.noaa.gov), is classified as high (>0.5), low (<−0.5) or average (between these two values) to characterize average atmospheric conditions in the Baltic Sea region (Vihma and Haapala, 2009).

RESULTS

Ice thickness, texture, stratigraphy and $\delta^{18}O$

There was considerable interannual variation of ice thickness, from 22 cm in 2005 to 60 cm in 2003 (Figs 1 and 2). There was no ice in 2008. All ice cores were composed of a granular ice layer overlying columnar ice. Some cores (four out of ten) had intermediate g/c layers sandwiched between granular and columnar layers. Granular ice layer thickness ranged from 1.5 to 20 cm. Columnar ice layer thickness ranged from 7 to 46 cm. Intermediate g/c ice thickness varied, when present, from 3 to 15 cm.

The ice $\delta^{18}O$ values varied between −14.7‰ and −4.9‰. The most negative values reflect the role of snow and/or rain in ice formation. For example, snow $\delta^{18}O$ values varied from −17.3‰ to −10.9‰, with an average of −14.5 ± 2.3‰. The least negative values, not as high as standard sea water (∼0‰), reflect mixing of sea water and fresh water to form the brackish water from which the columnar and intermediate g/c ice grow.

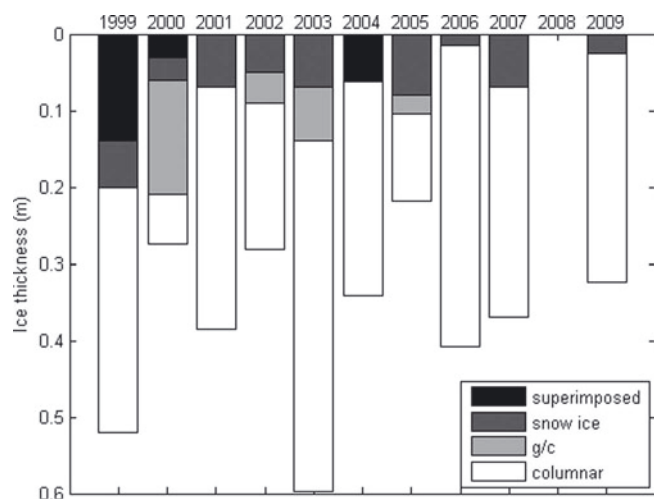**Fig. 2.** Ice thickness, texture/ice type and stratigraphy between 1999 and 2009. There was no ice in 2008.
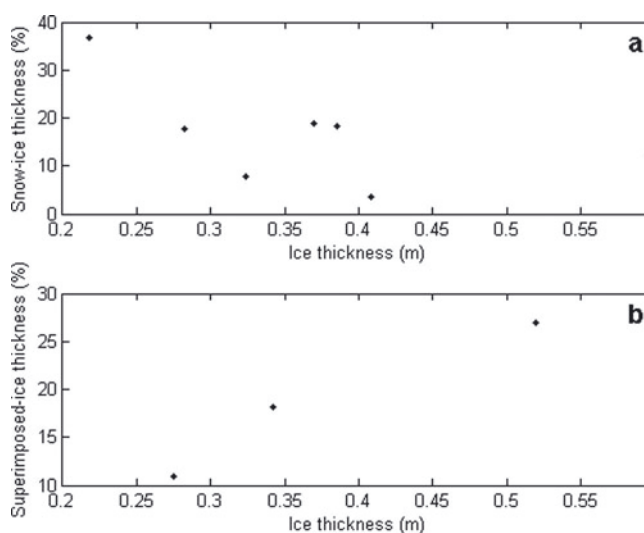

Fig. 3. Contribution of snow ice (a) and superimposed ice (b) to the total ice thickness. (a) includes only years with no superimposed-ice formation and (b) only years with superimposed-ice formation.

The most negative values in individual ice cores were found in the surface granular layers and primarily in the topmost layer (Figs 1 and 2). The exception was two ice cores (2004 and 2005) where the most negative values were in the granular layer immediately below the topmost layer. Below these topmost layers the $\delta^{18}O$ values increased steadily towards the bottom of the granular ice layers in all cores. The average granular ice $\delta^{18}O$ value was -10.1 ± 2.2‰.

In 50% of the cores, $\delta^{18}O$ values continued to increase through the columnar ice layers and the least negative values were observed in the bottommost layers. The increase towards the bottom is due to the decrease in columnar ice growth velocity as the ice thickens and increased isotopic fractionation during freezing (Tison and others, 2001). The other 50% of the cores had a maximum $\delta^{18}O$ value immediately beneath the granular layers, with a slight decrease in this value towards the bottom of the ice. This difference in $\delta^{18}O$ profiles was not dependent on the ice crystal texture, i.e. columnar or intermediate g/c ice. In intermediate g/c layers, $\delta^{18}O$ values were slightly more negative (average -6.4 ± 0.7‰) than in columnar ice layers (average -5.9 ± 0.4‰), most likely due to the difference in ice growth velocities as g/c ice layers were always above columnar ice layers.

The average columnar ice $\delta^{18}O$ values of each ice core (Table 1) were strongly correlated (correlation coefficient $r = 0.84$, p value 0.03) with the measured sea-water $\delta^{18}O$ value. The linear regression equation, water $\delta^{18}O = 1.32 \times$ ice $\delta^{18}O - 0.233$, made it possible, as described earlier, to estimate sea-water $\delta^{18}O$ values from columnar ice $\delta^{18}O$ values for the years when sea-water samples were lost. Average isotopic fractionation for all columnar ice layers in all cores was 2.2 ± 0.4‰.

Contributions of columnar ice, g/c ice, superimposed ice and snow ice

The contribution of columnar ice to the total ice thickness ranged from 24% to 96%, with an average of 71.5 ± 21.5% (mean ± std dev.). When present, the contribution of g/c ice to the total ice thickness ranged from 11.5% to 54.5%, with an average of 23.0 ± 21.1%. The granular ice contribution to total ice thickness was 3.7–38.5%, with an average of 19.3 ± 11.1%.

The granular ice layers were meteoric ice composed of snow ice or superimposed ice or both. The snow-ice contribution to total ice thickness varied between 0% and 36.7%, with an average of 13.7 ± 10.2%. Snow ice contributed all the meteoric ice in seven out of ten years and made a significant contribution to ice growth every year except 2004, when all the meteoric ice was superimposed ice. In those three years when the meteoric ice was composed of both snow ice and superimposed ice, they contributed >18% of total ice thickness. When present, superimposed ice contributed 10.9–26.9% of total ice thickness and 50–100% of meteoric ice.

The snow-ice contribution to total ice thickness was negatively correlated with total ice thickness ($r = -0.56$, p value 0.19), i.e. the thinner the ice cover the higher the snow-ice contribution (Fig. 3a). Conversely, the superimposed-ice contribution was positively correlated with total ice thickness ($r = 0.98$, p value 0.13), i.e. the thicker the ice cover the higher the superimposed-ice contribution (Fig. 3b).

Snow fraction

The snow fraction of the total ice thickness varied greatly, from 1.4% to 29.7%, with an average of 8.8 ± 9.3%. The highest values and the large range are due to the very high snow fraction in superimposed ice. When superimposed ice occurred, the average snow fraction (20.9 ± 7.8%) of the total ice thickness was much larger than in years with no superimposed ice (3.6 ± 2.1%). The average snow fraction in snow-ice layers was 33.3 ± 18.0%.

Influence of weather on ice thickness and composition

The NAO correlated with weather observations in the study area, and a higher NAO resulted in warmer, wetter and windier winters (Fig. 4). The measured temperature, precipitation and wind-velocity anomalies from 11 year (temperature and precipitation) or 9 year (wind) averages were well correlated to the NAO index. Early-winter (December–February (DJF)) average NAO has strong correlation to average early-winter precipitation ($r = 0.87$, p value 0.002) and good correlation to wind velocity ($r = 0.70$,
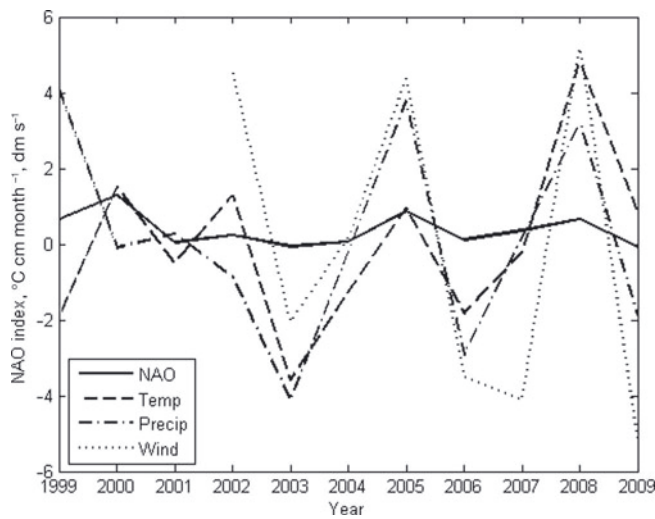
Fig. 4. Early-winter (DJF) mean NAO index and mean early-winter air temperature (°C), precipitation (cm month^{-1}) and wind velocity (dm s^{-1}) anomalies from 1999–2009 early-winter 11 year means. The anomalies are relative to 11 year DJF temperature, precipitation and wind averages of -1.5°C, 48.8 mm month^{-1} and 4.2 m s^{-1}, respectively.

Fig. 5. DJF NAO influence on meteoric ice contribution to total ice thickness, and JF NAO influence on total ice thickness.

p value 0.05) and temperature ($r = 0.62$, *p* value 0.07). The anomalies are relative to 11 year DJF temperature, precipitation and wind averages of -1.5°C, 48.8 mm month^{-1} and 4.2 m s^{-1}, respectively.

Total ice thickness was dependent on the mean January–February (JF) NAO index, i.e. high-JF-index winters had lower mean ice thickness (including 2008, when no ice formed) than years with average JF index ($r = -0.73$, *p* value 0.010) (Fig. 5). Note that the winter NAO was never classified as low (Fig. 4) during the study period. Ice composition was also well correlated with the NAO. The contribution of meteoric ice to the total ice thickness was correlated with the early-winter (DJF) mean NAO ($r = 0.81$,
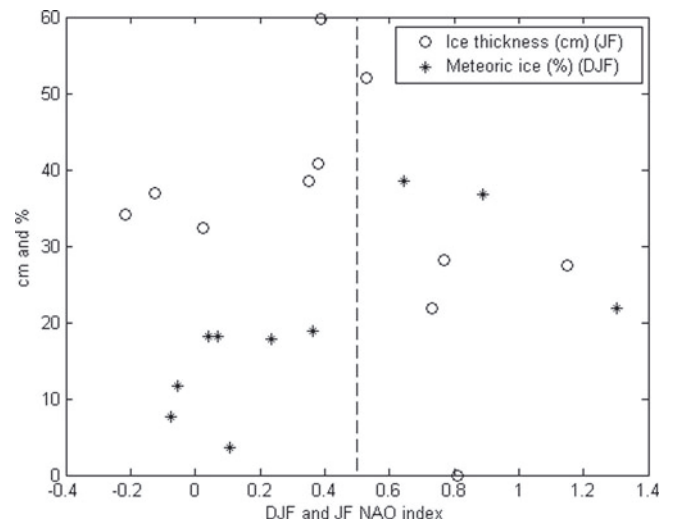
p value 0.005), i.e. years with high NAO values had a higher meteoric ice contribution than years with average NAO values, when mean contributions were 32.3% and 13.7%, respectively, of total ice thickness (Fig. 5). The intermediate g/c ice contribution was also correlated with the mean JF NAO, i.e. g/c ice made a much higher contribution to the total ice thickness in years with high NAO values (20.0% of ice thickness) than with average NAO values (2.0%).

Ice-thickness variation was largely due to freezing degree-days in early winter (Fig. 6a) ($r = -0.93$, *p* value 0.0001). Ice thickness correlated negatively with average winter temperature, precipitation and wind. Precipitation and wind are strongly positively correlated with temperature, which explains the relationship to ice thickness. A linear model to estimate ice thickness from early-winter FDD anomaly from the 11 year average (ice thickness $= -0.0026 \times$ FDD
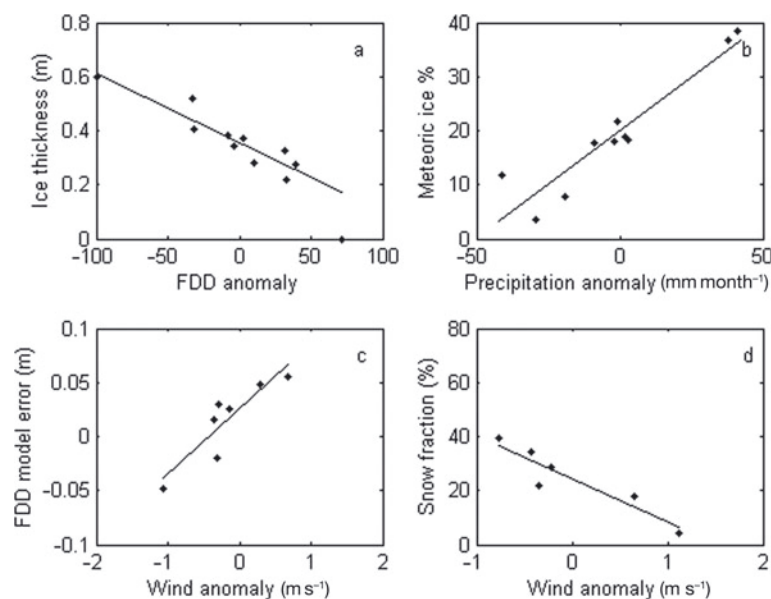

Fig. 6. Weather influence on ice thickness and properties: (a) FDD anomaly from 11 year early-winter mean and winter maximum ice thickness; (b) early-winter precipitation anomaly and meteoric ice contribution to total ice thickness; (c) January wind-speed anomaly and total ice-thickness error from FDD fit model; and (d) February wind-speed anomaly and snow fraction of meteoric ice. Regression lines are also shown; see text for equations.

anomaly + 0.3565) explained 86% of differences in ice thickness among the years. The 11 year DJF average was 83 freezing degree-days. The difference (residuals) between the linear model and observations was well correlated with wind speed (Fig. 6c) ($r = 0.90$, p value 0.006) (FDD model residual $= 0.061 \times$ wind anomaly + 0.026). Combining the FDD model and the wind-speed correction equation (ice thickness $= (-0.0026 \times$ FDD anomaly + 0.3565) $- (0.061 \times$ wind anomaly + 0.026)), annual ice thickness was estimated very well ($r = 0.993$, p value <0.0001), explaining 98% of the interannual variations in ice thickness from 2001 to 2009 (years with wind observations).

The contribution of meteoric ice to maximum ice thickness was strongly correlated with early-winter precipitation ($r = 0.94$, p value 0.0001); high precipitation resulted in a larger meteoric ice contribution to ice thickness (meteoric contribution $= 0.40 \times$ precipitation anomaly + 20.0) (Fig. 6b). The snow fraction in meteoric ice layers was well correlated with wind speed (Fig. 6d) ($r = -0.93$, p value 0.0063) (snow fraction $= -16 \times$ wind anomaly + 24), but not to precipitation or temperature. Winters with higher wind speeds also had thinner meteoric ice layers. Superimposed ice formation, which occurred only in some years, was associated with colder and wetter than average years.

DISCUSSION

In Santala Bay, ice stratigraphy showed typical Baltic Sea landfast ice characteristics, with a granular layer on top and intermediate g/c and columnar ice layers at the bottom (Kawamura and others, 2001; Granskog and others, 2003, 2004). The meteoric ice contribution (average 19.3%) to the ice thickness was typical of the Santala Bay area (Kawamura and others, 2001; Granskog and others, 2004), but considerably smaller than the 31.6% reported in Bay of Bothnia fast ice (Granskog and others, 2003). This difference is larger than interannual variation in Santala Bay samples and suggests that the difference is due to the spatial variability. The results also show that the contribution of meteoric ice to fast ice growth is at least as important in the Baltic Sea as in the Arctic Ocean (Gow and others, 1987) and the Okhotsk Sea (Toyota and others, 2004), where meteoric ice averages 10% of pack-ice thickness. However, meteoric ice is not as significant a factor in the Baltic Sea as it is in Antartica, where it contributes 24–27% of the total ice thickness (Jeffries and others, 1997).

The snow fraction of meteoric ice was highest when superimposed layers were observed, as it efficiently turns snow into ice. The average snow fraction of the total ice thickness, 8.8%, was less than the 18.3–20.7% reported in Bay of Bothnia fast ice (Granskog and others, 2003). This difference in snow fractions could be explained by higher superimposed-ice production in the Bay of Bothnia area, as there have been records of high superimposed-ice contributions (up to 22%) to the ice thickness (Granskog and others, 2006). Nevertheless, the results confirm that snow and meteoric ice play an important role in the mass balance of the Baltic Sea ice. The Santala Bay snow fractions are similar to the snow fractions reported in Antarctica, 3% (Eicken and others, 1994) and 4–15% (Jeffries and others, 1997), and indicate that meteoric ice formation processes are similar in these two very different regions.

The thicker the Santala Bay ice cover, the smaller the contribution of snow ice, and vice versa. Eicken and others

(1994) made a similar observation in the Weddell Sea, Antarctica, noting that, although snow ice contributes significantly to the ice thickness, the overall effect of snow on ice is to reduce the level-ice thickness because the insulating effect of the snow outweighs the consequences of snow mass and snow-ice formation. The superimposed-ice contribution was also related to the total ice thickness and can be higher in thicker ice. This is probably because thicker ice can support a deeper, heavier snow cover without flooding and snow-ice formation, with superimposed-ice accumulation then occurring when the conditions for its formation (melting and refreezing of the snow alone, or freezing of rain-soaked snow) are met (Granskog and others, 2006).

High winter NAO values are typically associated with windy, warm and moist weather in the Gulf of Finland (Vihma and Haapala, 2009). A thinner ice cover and larger granular/meteoric ice contribution to total ice thickness are a logical consequence of high-NAO weather patterns. Higher temperature means lower basal freezing rates and less columnar ice growth, while higher precipitation creates suitable conditions for snow-ice accumulation after flooding and/or superimposed-ice accumulation due to melting in the snow cover or percolation of rain through the snow to the ice surface.

Of all the weather parameters, FDD had by far the greatest influence on total ice thickness. A linear FDD–ice-thickness model explains most of the variance in ice thickness, despite the complicating effects of snow-ice and superimposed-ice growth. Neither meteoric ice thickness nor its contribution to total ice thickness was well correlated with temperature or FDD. This is probably because they are second-order effects in meteoric ice accumulation, which, especially in the case of snow ice, depends in the first instance on having sufficient mass of snow to cause flooding.

The thickness and mass of the snow cover also depend on the wind, which probably explains some of the variance in the FDD–ice-thickness relationship (Fig. 6c), and variation in the amount of meteoric ice, as higher wind velocities resulted in smaller ice thicknesses than the FDD model estimated and also thinner meteoric ice layers than precipitation amounts predicted. These effects relate to snow transport and the accumulation or deflation of snow and thus whether there is sufficient mass of snow to cause flooding and snow-ice formation. Changes in the production of meteoric ice layers, due to the changes in snow mass on ice, are not compensated with changes in basal ice growth rates if the insulating properties of the snow cover do not change accordingly. Low-density depth-hoar snow layers can alter these insulation properties so that a thinner snow layer does not result in less insulation.

Lower snow fractions in meteoric ice layers were also associated with higher wind speeds (Fig. 6d). This also suggests lower densities at the bottom of snow cover, which can be explained by low air temperatures and steep, negative temperature gradients in thin snow cover which cause low-density depth hoar to form at the base of an otherwise dense, wind-packed snow cover.

Combined FDD and wind-speed effect equations provide very good ice-thickness estimates for this area. This addition of wind-related snow processes to the FDD model emphasizes the importance of snow-related effects to the ice-thickness evolution. It is also clear that wind- and

snow-related processes can vary significantly from place to place and make it inaccurate to estimate ice thicknesses based solely on our simple equation. To properly make a FDD and wind fit to each location requires multiple ice measurements from the location, thus making numerical models a more appropriate means to capture quantitative spatial and temporal variation of meteoric ice formation (Cheng and others, 2006).

CONCLUSIONS

In the Baltic Sea, the 82.0% contribution of columnar and intermediate g/c ice to the total landfast ice thickness indicates that thickening is dominated by downward thermodynamic ice growth at the bottom of the ice cover. Snow ice, which contributes 12.4% of the total ice thickness, is the second most important thickening process. Only occasionally does superimposed ice contribute significantly to thickening the ice cover. The snow entrained in the snow-ice and superimposed-ice layers combined makes up 8.8% of the total ice mass. The thicker the ice cover is, the lower the contribution of meteoric ice growth to ice thickness, indicating that, although meteoric ice is a significant contributor to the ice thickness, the overall effect of snow on the ice is to decrease the total ice thicknesses due to insulation and reduced basal growth rates.

Weather affected the ice thickness and the meteoric ice contribution to landfast ice. Early-winter (DJF) average temperature, and especially the sum of freezing degree days, explained much of the variance in maximum ice thickness. Average early-winter precipitation was a good indicator for meteoric ice contribution to the maximum ice thickness, with higher precipitation leading to higher contribution of meteoric ice. Superimposed-ice formation was connected to certain weather patterns, with cold, wet winters more likely to produce superimposed ice than average or warm winters. Higher wind speeds appear to lead to less snow being entrained in meteoric ice and thus a smaller snow contribution to total ice mass.

Future climate in the Baltic Sea area is expected to be warmer and wetter (Rutgersson and others, 2002). The results of this study suggest that this will lead to thinner ice covers with a higher proportion of meteoric ice, especially snow ice. However, in sufficiently warm weather, landfast sea ice will not form at all on the southern coast of Finland.

ACKNOWLEDGEMENTS

REFERENCES

Cheng, B., T. Vihma, R. Pirazzini and M.A. Granskog. 2006. Modelling of superimposed ice formation during the spring snowmelt period in the Baltic Sea. *Ann. Glaciol.,* **44**, 139–146.

Eicken, H. and M.A. Lange. 1989. Development and properties of sea ice in the coastal regime of the southeastern Weddell Sea. *J. Geophys. Res.,* **94**(C6), 8193–8206.

Eicken, H., M.A. Lange, H.W. Hubberten and P. Wadhams. 1994. Characteristics and distribution patterns of snow and meteoric ice in the Weddell Sea and their contribution to the mass balance of sea ice. *Ann. Geophys.,* **12**(1), 80–93.

Gow, A.J., W.B. Tucker, III and W.F. Weeks. 1987. Physical properties of summer sea ice in the Fram Strait, June–July 1984. *CRREL Rep.* 87-16.

Granskog, M.A., T.A. Martma and R.A. Vaikmäe. 2003. Development, structure and composition of land-fast sea ice in the northern Baltic Sea. *J. Glaciol.,* **49**(164), 139–148.

Granskog, M.A., M. Leppäranta, T. Kawamura, J. Ehn and K. Shirasawa. 2004. Seasonal development of the properties and composition of landfast sea ice in the Gulf of Finland, the Baltic Sea. *J. Geophys. Res.,* **109**(C2), C02020. (10.1029/2003JC001874.)

Granskog, M.A., T. Vihma, R. Pirazzini and B. Cheng. 2006. Superimposed ice formation and surface energy fluxes on sea ice during the spring melt–freeze period in the Baltic Sea. *J. Glaciol.,* **52**(176), 119–127.

Jeffries, M.O., R.A. Shaw, K. Morris, A.L. Veazey and H.R. Krouse. 1994. Crystal structure, stable isotopes (δ^{18}O), and development of sea ice in the Ross, Amundsen, and Bellingshausen seas, Antarctica. *J. Geophys. Res.,* **99**(C1), 985–995.

Jeffries, M.O., A.P. Worby, K. Morris and W.F. Weeks. 1997. Seasonal variations in the properties and structural composition of sea ice and snow cover in the Bellingshausen and Amundsen Seas, Antarctica. *J. Glaciol.,* **43**(143), 138–151.

Kawamura, T. *and 9 others.* 2001. Time-series observations of the structure and properties of brackish ice in the Gulf of Finland. *Ann. Glaciol.,* **33**, 1–4.

Lange, M.A., P. Schlosser, S.F. Ackley, P. Wadhams and G.S. Dieckmann. 1990. ^{18}O concentrations in sea ice of the Weddell Sea, Antarctica. *J. Glaciol.,* **36**(124), 315–323.

Macdonald, R.W., E.C. Carmack and D.W. Paton. 1999. Using the δ^{18}O composition in landfast ice as a record of arctic estuarine processes. *Mar. Chem.,* **65**(1–2), 3–24.

Palosuo, E. 1963. The Gulf of Bothnia in winter. II. Freezing and ice forms. *Merentutkimuslaitoksen Julkaisu/Havsforskningsinst. Skr.,* **209**, 42–64.

Rutgersson, A., A. Omstedt and J. Räisänen. 2002. Net precipitation over the Baltic Sea during present and future climate conditions. *Climate Res.,* **22**(1), 27–39.

Tison, J.L., A. Khazendar and E. Roulin. 2001. A two-phase approach to the simulation of the combined isotope/salinity signal of marine ice. *J. Geophys. Res.,* **106**(C12), 31,387–31,401.

Toyota, T., T. Kawamura, K.I. Ohshima, H. Shimoda and M. Wakatsuchi. 2004. Thickness distribution, texture and stratigraphy, and a simple probabilistic model for dynamical thickening of sea ice in the southern Sea of Okhotsk. *J. Geophys. Res.,* **109**(C6), C06001. (10.1029/2003JC002090.)

Vihma, T. and J. Haapala. 2009. Geophysics of sea ice in the Baltic Sea: a review. *Progr. Oceanogr.,* **80**(3–4), 129–148.